Optical Properties of Excitons Bound to Neutral Acceptors in GaP

P. J. Dean,† R. A. Faulkner, S. Kimura,* and M. Ilegems
Bell Telephone Laboratories, Murray Hill, New Jersey 07974
(Received 11 December 1970)

Luminescence of excitons bound to five point defects and one complex neutral acceptor has been identified in GaP. These excitons are weakly bound, and have weak no-phonon lines because of the symmetry of the electron in the exciton. The high degeneracy of this electron in GaP, resulting from the multivalleyed conduction band, together with the allowed states for the combination of two $j=\frac{3}{2}$ holes, gives 12 possible distinct no-phonon lines in the exciton transition, many of which have been seen for the shallower acceptors. These bound excitons obey a modified form of Haynes's rule. This fact, the magnitude of the exciton localization energies and the magneto-optical properties of these excitons firmly establish the nature of these transitions. Mirror symmetry is exhibited between the absorption and luminescence spectra of the Zn exciton, and the time for radiative decay has been determined. This is 500 times longer than the measured luminescence decay time, because of the predominance of the Auger recombination channel. The radiative decay times of these shallow excitons are nearly independent of the acceptor. The dependence of the Auger lifetimes τ_E on the binding energies of the exciton complexes have been established for the first time. It is shown that $\tau_E \propto E_A^n$, where $n \sim -4.5$, close to the value (-4.0) predicted from a hydrogenic model with a single spherical valence band. It is clear that deeper (neutral) acceptors form highly nonradiative recombination centers for excitons, with very short decay times. Strong complex satellites in the acceptor-exciton luminescence may involve phonons associated with the dynamic Jahn-Teller effect. Weaker "two-hole" luminescence transitions have been tentatively identified for the Zn and Cd acceptors. If this identification is correct, different types of final hole states are seen for these two acceptors.

I. INTRODUCTION

Electronic transitions associated with isolated acceptors in GaP were only recently observed and identified,[1] although the shallow acceptors have been long recognized in the luminescence of donor-acceptor pairs.[2] In addition, the radiative decay of excitons on neutral donors was the subject of an early study.[3] Theory predicts that a finite binding energy should also exist for excitons at neutral acceptors,[4] and it was expected that luminescence due to the decay of this exciton should occur.

The observation and, in particular, a detailed study of the luminescence or absorption of acceptor-exciton complexes in GaP are made difficult by several inherent properties. The band structure of GaP is such that the radiative decay rate of electronic states whose binding energy is primarily due to the interaction of holes with impurities is small compared with states associated with electron-attractive P-site impurities. The decay of excitons at neutral acceptors is very similar in this respect to that of excitons at neutral Ga-site donors.[5] In addition, it happens that the localization energy E_{BX}[6] of excitons at typical neutral acceptors is significantly less than for excitons bound to typical neutral donors. This is true even for donors and acceptors with comparable binding energies E_D and E_A. The luminescence of these very shallow bound-exciton states is readily quenched by tunneling of the excitation energy (exciton) to deeper states before radiative decay can occur. In addition, typical acceptors are shallower than typical donors in GaP. This implies a relatively low hole-acceptor ion interaction, which further reduces the oscillator strength of no-phonon decay of the bound exciton as described in Sec. III A. The effect of these considerations is that the optical spectra of excitons bound to neutral acceptors in GaP contain *very weak* no-phonon lines. In consequence, crystals containing optimally large concentrations of neutral acceptors with minimal concentrations of P-site donors such as S and isoelectronic traps like N are a prerequisite to the detailed study of acceptor-exciton complexes in GaP. We single out S and N since they, together with O, C, and, under certain conditions, Si, are the predominant inadvertently present impurities in GaP.

In this paper, we report detailed studies of the optical properties of excitons bound to six different neutral acceptors in GaP, following the preliminary report of the observation and identification of this decay mechanism in GaP.[1] Crystal growth is described in Sec. II A and experimental techniques of luminescence-spectral and lifetime measurements in Sec. II B. The form of the luminescence spectrum and its dependence on the acceptor is discussed in Sec. III A. In Sec. III B, we show from a detail study of the no-phonon components in these exciton spectra and their behavior in a magnetic

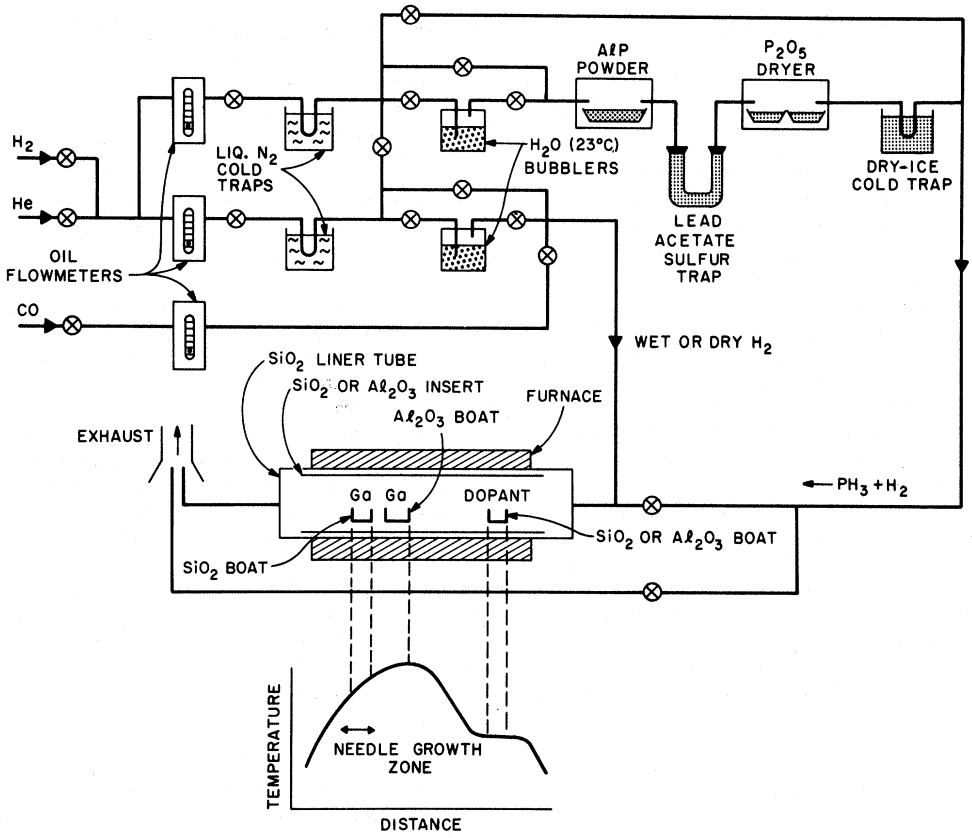

FIG. 1. Open-tube furnace system used to grow the deliberately doped GaP crystals with the low concentrations of unwanted impurities needed for the study of the weak optical properties of excitons bound to neutral acceptors. Crystals grown in the Ga solution in the central boat and downstream by vapor transport were used.

field that the high degeneracy possible for these bound excitons is substantially lifted by j-j coupling and, probably, crystal field interaction in zero magnetic field. Thus, many no-phonon lines occur, very closely spaced for shallow effective-mass-like acceptors such as C. Observation of the weak absorption of the Zn-exciton complex (Sec. III C) enables the oscillator strength and radiative lifetime to be calculated. The experimental lifetimes reported in Sec. III C are much shorter than the calculated radiative lifetimes. As has been done for the corresponding exciton-donor complexes,[7] we attribute the speedup of the transition rate to the predominance of nonradiative (Auger) decays. The lifetimes previously reported for the Zn acceptor[1] are slightly revised. In addition, observation of these lifetimes over a range of E_A and the exciton localization energy E_{BX} provides significant new evidence of the systematics of Auger transition rates in semiconductors. Weak satellites occur in the Zn- and Cd-exciton spectra at positions consistent with those "two-hole" components predicted to be the most prominent. Stronger satellites observed for all excitons except Cd probably involve low-energy localized vibrations characteristic of interactions with the ground state of neutral acceptors in GaP.

II. EXPERIMENTAL

A. Crystal Growth

GaP crystals doped with the acceptors C, Zn, Cd, Hg, Mg, and X (unknown) were grown from Ga solution or from the vapor phase in the open-tube furnace system shown in Fig. 1. This system, a modification of the one described by Dean, Frosch, and Henry,[8] consists essentially of quartz reaction apparatus containing a Ga boat which is heated to temperatures in the range 1060–1100 °C, over which the source of P is a controlled flow of PH_3. Purified H_2, either dry or containing a determined amount of H_2O vapor, is used as the carrier gas, while the dopant impurities are introduced either (a) directly from the gas phase (e.g., CO), (b) from metallic sources placed in a low-temperature zone upstream of the region of crystal growth (e.g., Zn, Cd, Hg, Mg), or (c) by adding the impurity in elemental (e.g., Mg) or compound (e.g., Mg_3N_2) form directly to the Ga charge.

The growth system and the experimental opera-

tion conditions are designed to minimize contamination by other than the desired acceptor impurities. To this end, the H_2 carrier gas is purified by passage through a palladium-silver alloy diffuser and the PH_3 is generated *in situ* by passing wet H_2 over powdered AlP, the Frosch process.[9] Liquid-N_2 cold traps are used to reduce the possibility of C contamination from the oil used in the gas-flow meters and to further purify the carrier gases admitted to the system. To remove S, which is a common impurity in the AlP and is liberated as H_2S, a trap containing $Pb(C_2H_3O_2)_2 \cdot 3H_2O$, either in powder form or as a saturated solution in water, is placed in series with the gas stream. A Cellosolve acetate-CO_2 cold trap at approximately -77 °C, preceded by an optional P_2O_5 dryer tube, is used to reduce the concentration of unreacted water, acetic acid formed by reaction between lead acetate and H_2S, and other residual impurities. Finally, a flow of dry He is maintained continuously in the system between successive runs and a minimum purge period of 16 h is observed each time the system is opened to air to replenish the AlP source and the $Pb(C_2H_3O_2)_2 \cdot 3H_2O$ and P_2O_5 traps.

GaP needles doped with the elements Zn, Cd, and Hg were grown by the water-vapor transport method. In this method the GaP formed in the Ga boat in the high-temperature zone is transported by the reaction

$$2GaP(s) + H_2O(g) \rightarrow Ga_2O(g) + H_2(g) + P_2(g), \quad (1)$$

where the state, either solid or gas, is given in parenthesis after the material. Gallium phosphide needles are regrown downstream in a 960–1040 °C temperature zone by reaction between Ga_2O and P_2. The acceptor doping levels were controlled by varying the temperature of the boat containing the dopant elements. Optimal exciton spectra were obtained by adopting dopant temperatures of, respectively, 400 °C for Zn, 500 °C for Cd, and 290 °C for Hg. Under these conditions, doping levels in the $10^{16} \rightarrow 10^{17}$-$cm^{-3}$ range were typically obtained, except for Hg, where successful doping was not achieved.

The yield of the vapor transport and the size of the grown needles depend critically on the furnace configuration and on the flow rates. Typically, flow rates were around 260 cc/min for the $H_2 + PH_3$ and 140 cc/min for the $H_2 + H_2O$ gas mixtures, the optimum values being chosen empirically. A small additional Ga boat in the needle-growth zone increased the needle yield and size appreciably, with the most massive needles originating at the upstream end of the boat. Under these conditions, needles ~1 mm thick and $\gtrsim 1.5$ cm long were commonly obtained in a 3–5 h run.

Through the presence of H_2O vapor in the system, Si contamination from the quartz liner and insert tubes as well as contamination from other uncontrolled easily oxidizable impurities such as C are reduced to negligible levels, $\lesssim 10^{15}$ cm^{-3}. In addition, it was found that the vapor-grown needles contained concentrations of the persistent impurities N and S at only about 10% of the typical values in GaP platelets grown in Ga solution during the same runs. Since N and S induce prominent near-gap optical transitions in GaP that can readily mask the acceptor-induced spectra, vapor-grown GaP was the preferred material in this study. Typically, residual N and S levels determined by optical absorption were $\lesssim 10^{14}$ cm^{-3} and $\lesssim 10^{15}$ cm^{-3}, respectively, in the needles.

The reactivity of C and Mg with O precludes the growth of GaP needles doped with these elements by the water-vapor transport method. Solution-grown crystals doped with C were, however, conveniently obtained by adding CO to a dry $PH_3 + H_2$ gas stream. The C doping level was controlled by the CO flow rate, which was set at about 10% of the total flow rate given above. For Mg, the doping levels could not be controlled readily by this technique because of oxide formation. In fact, the Mg-exciton spectra were best observed in crystals that were not advertently doped with Mg, but rather had been grown from Ga solutions to which $CaCl_2$ had been added as a dopant in a dry $PH_3 + H_2$ atmosphere. The Mg spectra were successfully reproduced first by simply adding Mg to the Ga charge or by placing elemental Mg upstream at 450 °C, and later with better control by adding Mg_3N_2 to the Ga charge. Usually, these Mg doping techniques were used to produce solution-grown crystals for the study of donor-acceptor pair spectra involving the acceptor Mg, reported elsewhere.[10] Strong Si-Si donor-acceptor pair emission was usually observed in the crystals grown in the absence of water vapor, especially in those doped by introducing Mg from the vapor phase, because of the reduction reaction taking place at the walls of the SiO_2 insert tube. The unidentified acceptor X was observed in non-intentionally doped crystals grown from Ga solution in the presence of water vapor, as previously reported.[11]

In view of the problems encountered with Mg doping, in-growth doping with Be was not attempted. Rather, this acceptor was introduced by diffusion from a liquid Ga-Be-P solution into selected GaP substrates.[12] The best Be-exciton spectra were observed following diffusion for 1 h at 750 °C into undoped GaP needles, grown as discussed above. The diffusion depth under these conditions is of the order of 25 μ, comparable to the penetration depth of the exciting light (Sec. IIB).

B. Optical Measurements

Luminescence spectra of the acceptor-exciton

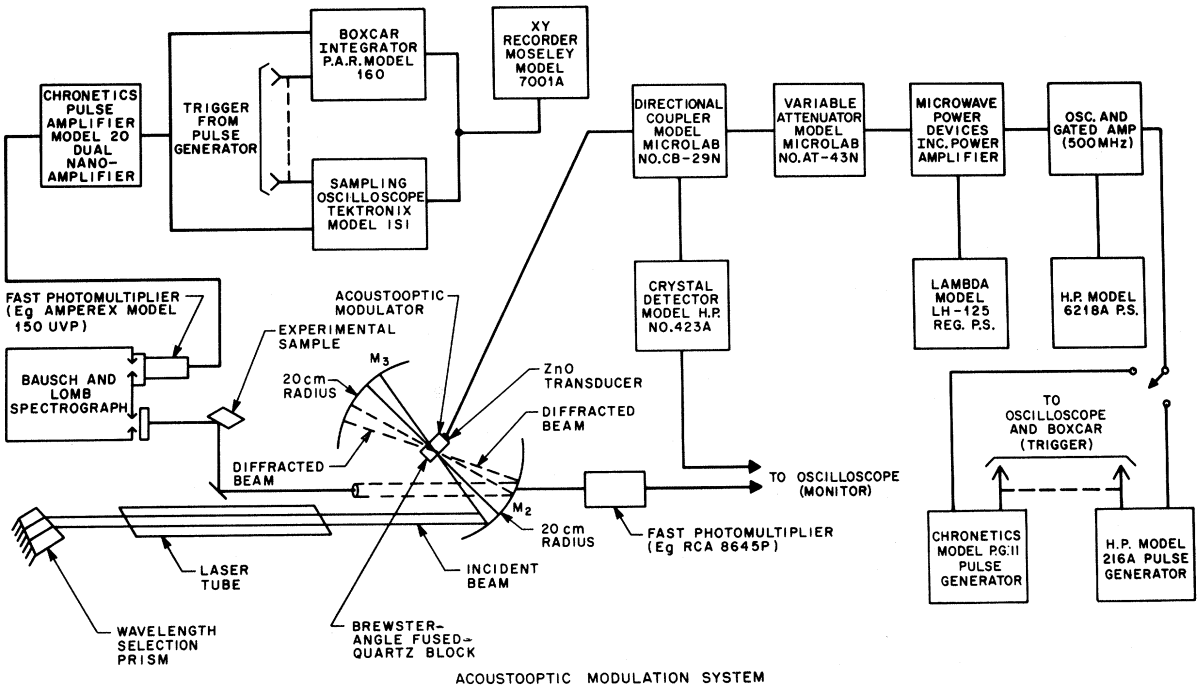

FIG. 2. Schematic diagram of the intracavity acousto-optic modulation system used with an Ar^+ laser to measure the lifetimes of the fast, inefficient, luminescence of excitons at neutral acceptors in GaP.

complexes were recorded photographically with a 2-m f/17 Bausch and Lomb spectrograph from freely suspended crystals immersed in liquid He, generally pumped below the λ point. The luminescence was excited by 4880-Å light from an Ar^+ laser. Zeeman spectra were obtained using either a 12-in. Varian electromagnet (up to 30.5 kG) with the Bausch and Lomb spectrograph or a Westinghouse 50-kG superconducting solenoid with a 1-m Jarrell-Ash spectrograph.

The luminescence decay times of transitions from the lower-energy states of these complexes were measured at 1.6 °K using the system shown in Fig. 2. A small fraction (few percent) of the instantaneous cavity power was coupled out by Bragg diffraction from the ultrasonic elastic waves launched into the quartz deflector block from the ZnO transducer.[13] The lifetimes of the excitons described here are short, $\lesssim$300 nsec. Therefore, the HP No. 216A rf oscillator was used to drive the transducer. With a pulse repetition rate of a few MHz and a pulse length of ~10 nsec, the time-average laser output power was over 30% of that available from the same Ar^+ laser operated in conventional cw mode with the deflector and short-focus cavity mirrors replaced by a standard long-focus 3% transmission output mirror. With this efficient pulsed excitation system, the lifetimes of the fast inefficient acceptor-exciton luminescence in GaP could be adequately measured with the Tektronix 1S1 sampling plug-in connected to function as a boxcar integrator of fixed gate width.

Absorption spectra of crystals doped much more heavily with Zn (~10^{18} cm^{-3}) than the lightly doped crystals used for the luminescence studies were measured with a $\frac{3}{4}$-m f/6.8 Spex 1401 scanning monochromator using a tungsten light source. Transmission studies on vapor-grown needles 5–6 mm long were necessary for accurate measurements of the weak absorption induced by neutral acceptors, even at these high concentration levels. The crystals were cooled to ~20 °K in a stream of cold He gas. Absorption of the Cd exciton was also detectable in long vapor-grown needles.

III. RESULTS AND DISCUSSION

A. Luminescence Spectra of Neutral Acceptors

The luminescence in Fig. 3 is almost entirely due to the decay of excitons bound to the acceptor Zn. The fact that this spectrum is invariably and exclusively seen in refined GaP crystals in the presence of light Zn doping, optimally ~10^{16}–10^{17}-cm^{-3} neutral Zn acceptors, strongly suggests that Zn is involved in these electronic transitions. Above ~10^{17}-cm^{-3} neutral Zn acceptors, lower-energy luminescence due to electronic transitions at Zn-S pairs becomes significant. The shallow exciton luminescence eventually quenches in favor of the pair luminescence because of capture competition

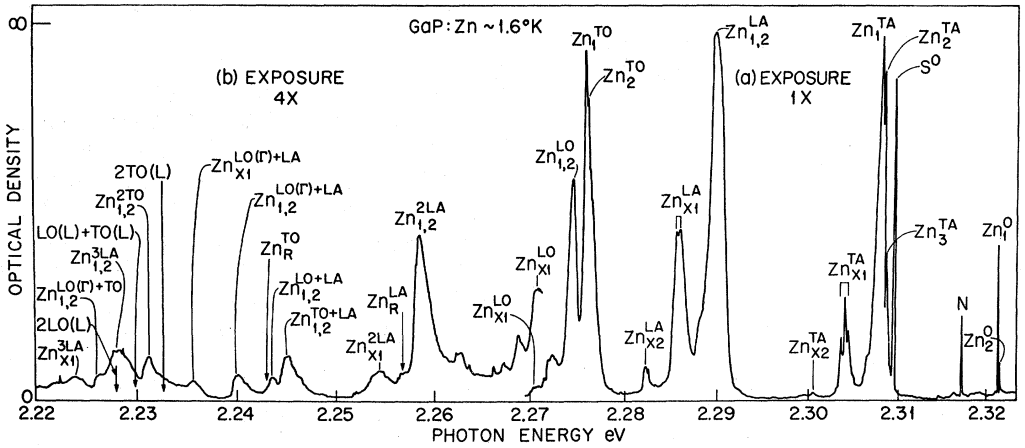

FIG. 3. Photoluminescence spectrum of excitons bound to neutral Zn acceptors at low temperature, recorded photographically from a vapor-grown needle. The TA-, LA-, and TO-MC phonon replicas are overexposed to show the weak no-phonon components $Zn^0_{1,2}$. Phonons other than MC are identified explicitly, e.g., $\vec{k}=0(\Gamma)$ and L. The multiphonon components (below ~2.27 eV) and the satellite components $Zn_{X1,X2}$ are discussed in the text. Components N and S^0 are due to residual N and S.

and the tunneling process mentioned in Sec. I.

The relative positions of the principal lines, shown heavily overexposed in Fig. 3, indicate that they correspond to exciton decay with the emission of the TA, LA, TO, and LO phonons, which conserve momentum in the indirect transition [momentum conserving (MC) phonons]. The relatively weak lines $Zn^0_{1,2}$ arise from no-phonon recombinations. It is shown in Sec. IIIB that up to 12 no-phonon lines may appear in such acceptor-exciton spectra in GaP. Gallium phosphide is an indirect-gap semiconductor with conduction-band minima close to, or most probably at,[14] the ⟨100⟩ zone boundary points in the reduced zone, symmetry point X. The degenerate valence-band maximum occurs at the zone center, symmetry point Γ. Then, the energies of the MC phonons correspond to phonons of wave vector $\vec{k}_{phon} \sim \vec{k}_x - \vec{k}_\Gamma \sim \vec{k}_x$. The energies of the four phonons obtained using the assignments given in Fig. 3, together with values for three other acceptors, are compared with previous estimates for MC phonons in GaP in Table I of Ref. 5 and good agreement is found.

The spectrum in Fig. 3 was obtained from a crystal containing 3×10^{16}-cm^{-3} neutral Zn acceptors, with $\lesssim 10^{14}$-cm^{-3} N isoelectronic traps. The acceptor-exciton states are very diffuse; the localization energy E_{BX} of the exciton on neutral Zn acceptors is only ~6.65 meV. As we have seen, sharp acceptor-exciton luminescence spectra can be obtained only when the relative and absolute concentrations of optically active inadvertent impurities is sufficiently low that excitation tunneling out of the Zn-exciton states before recombination is improbable. This is a stringent requirement because of the diffuse nature of these states.

The low value of $E_g - (h\nu)\,Zn^0_1$, ~17 meV, provides the first indication that the exciton is bound to a *neutral* Zn acceptor, since this energy must significantly exceed $(E_A)_{Zn}$, i.e., be > 64 meV,[10] if the exciton were bound to an ionized acceptor. This assignment is consistent with the magneto-optical properties of Zn^0_1 (Sec. IIIB). Additional support for this assignment is obtained in Fig. 4, where E_{BX} is shown to be accurately proportional to the ionization energy for the five-point defect acceptors in GaP for which exciton transitions have been recognized.[15] The values of E_{BX} for the six acceptor-exciton complexes reported here are listed in Table I.

A linear relationship between E_{BX} and E_A is expected from perturbation theory for small increases in E_{BX} above the value $(E_{BX})_{EM}$ for an exciton bound to a neutral effective-mass acceptor. Such a relationship implies that the exciton is bound by the exchange interaction between the two like particles (holes in the present examples) rather than, for example, by polarization forces. This fact was rec-

TABLE I. Electronic energies from acceptor-exciton complexes in GaP.

Acceptor	E_{BX}[a] (meV)	ΔE (meV) High-energy satellites	ΔE (meV) Low-energy satellites
X	5.1	4.8; 8.3 (X_X)	
C	5.77	3.9; (C_X)	
Be	5.9	4.1; 7.4 (Be_X)	
Mg	6.0	3.6; 7.2 (Mg_X)	
Zn	6.65	4.1; 7.6 (Zn_X)	33.3 ($Zn_R^{LA,TO}$)
Cd	8.4		82.5 (Cd_1^{2H})

[a]From the free-exciton gap, $E_{gx}=2.328$ eV.

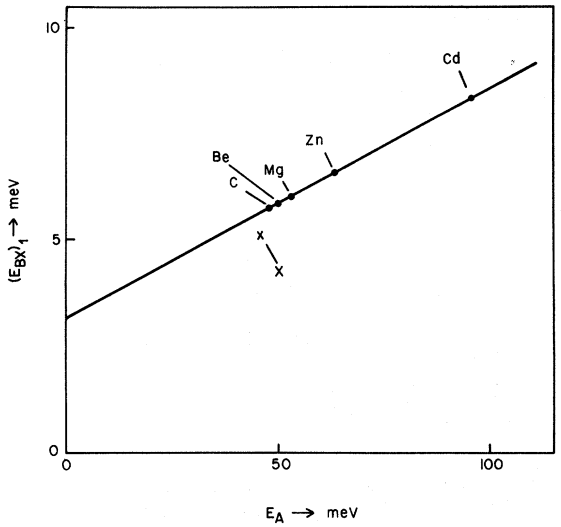

FIG. 4. Dependence on the acceptor ionization energy of the localization energy for the lowest no-phonon component in the luminescence of excitons bound to neutral acceptors in GaP. Acceptors C, Be, Mg, Zn, and Cd are point defects, X is an unidentified complex.

ognized by Haynes in his discussion of the first experimental proof of the existence of these complexes (in Si [16]), confirming an earlier theoretical prediction by Lampert.[17] However, the relationship observed both for donor and acceptor complexes in Si is extrapolates back to pass near the point $E_{BX} = 0$, E_D or $E_A = 0$, and has become known as Haynes's rule in this form. Figure 4 shows that E_{BX} is definitely nonzero (~ 3.5 meV) when $E_A = 0$ for the acceptor complexes in GaP. If we treat the two holes on an equal footing, we may write

$$E_{BX} = \alpha (E_A)_{EM} + \beta (E_A)_{CC}$$
$$= (\alpha - \beta)(E_A)_{EM} + \beta E_A . \quad (2)$$

We recognize explicitly in Eq. (2) two essentially distinct contributions to E_A, namely, $(E_A)_{EM}$ due to the Coulomb interaction of the hole with the acceptor ion charge, screened by the dielectric response of the lattice, and $(E_A)_{CC}$, usually called the central-cell contribution to the binding, arising from non-Coulombic interactions with the hole wave function in the vicinity of the central cell. We further recognize that changes in E_A due to small perturbations in these two essentially distinct interaction potentials should generally produce quantitatively different changes in E_{BX}. These changes are described by the coefficients α and β.

For a sequence of acceptors in a given semiconductor, changes in E_A are governed by the coefficient β, and the term $(\alpha - \beta)(E_A)_{EM}$ in Eq. (2) is a constant. This constant is zero only if $\alpha = \beta$, as seems to be so for the common donors and acceptors in Si.[16] From Fig. 4, $\alpha - \beta$ is positive and $\alpha/\beta \sim 2.5$ for acceptor-exciton complexes in GaP. We conclude that the localization energy of these excitons is more influenced by the over-all wave function of the first hole to be bound than by the central-cell interaction. Reasons why GaP differs so markedly from Si in this respect will be discussed elsewhere. Previously reported[5] and more recent data on the relationship between E_{BX} and E_D for excitons bound to neutral donors in GaP also indicates that $E_{BX} \neq 0$ when $E_D = 0$.[18]

The bound-exciton luminescence characteristic of GaP doped with Cd, Be, Mg,[19] and C acceptors is shown in Figs. 5–8.[20] No evidence was obtained for optical transitions associated with the potential acceptor Hg in crystals grown in the presence of the highest usable partial pressure of Hg (Sec. II A). We conclude that Hg is very insoluble, presumably due to size mismatch. However, if the acceptor Hg is significantly deeper than Cd, following the trend established for the group-II acceptors (Table III), Hg-exciton luminescence would be hard to detect because of the large branching ratio in favor of Auger recombination (Sec. III C). Studies of donor-acceptor pair luminescence [2,10] unambiguously show that these acceptors are all point defect substituents on the Ga(Be, Mg, Zn, Cd) or P(C) host lattice sites. As far as can be determined, the exciton spectra are qualitatively very similar, with relatively weak no-phonon lines, and strong MC one-phonon replicas. Multiphonon replicas also occur, in which components involving second and third interactions with the LA-MC phonon are dominant. In addition replicas of MC one-phonon components which involve interactions with the long-wavelength TO and LO phonons are prominent. The phonon energies used in Fig. 3 and Figs. 5–8 are given in Table II. Essentially all the clearly resolved low-energy components are accounted for by these multiphonon processes, when the phonon sidebands of the satellite lines Zn_x, Mg_x, Be_x, and C_x are also recognized. These satellites are an integral part of the exciton luminescence spectra of these acceptors. Their origin is discussed below. In particular, there is no evidence for strong multiple phonon-assisted transitions involving L ($\langle 111 \rangle$ zone boundary) phonons (Fig. 3), which are allowed

TABLE II. Phonon energies in acceptor exciton spectra in GaP.

Momentum conserving		Other	
Phonon	Energy (meV)	Phonon	Energy (meV)
TA	13.1	LO(Γ)	50.0
LA	31.7	LO(L)	46.8
TO	45.4	TO(L)	44.8
LO	46.8		

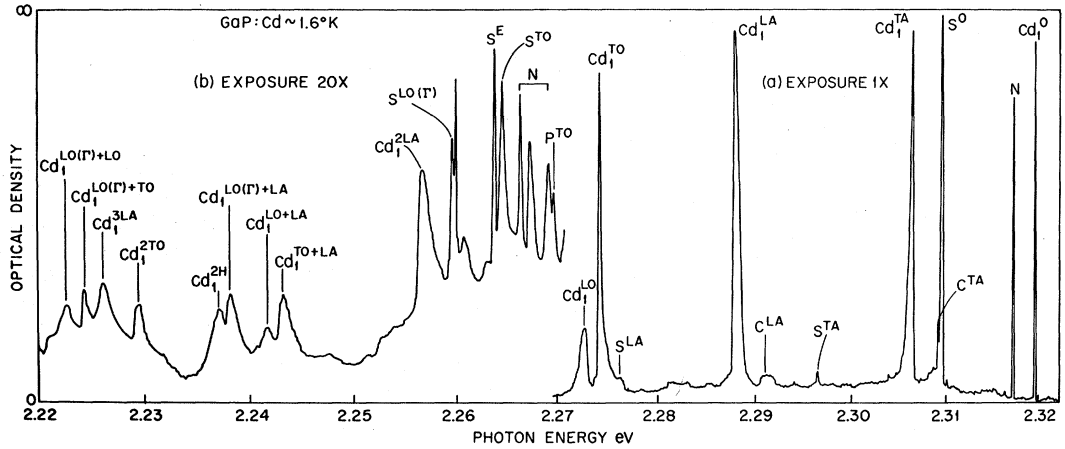

FIG. 5. Low-temperature photoluminescence spectrum of excitons bound to neutral Cd acceptors in GaP, recorded photographically from a vapor-grown needle. Notation as in Fig. 3, components C^{TA}, etc., are due to residual C.

by symmetry, consistent with the spectra of excitons bound to the shallow Ga-site donor Sn.[5]

The distinctive sawtooth shape of components associated with the LA phonon is preserved even in the multiphonon replicas. The low- (optical transition) energy side of this component exhibits a sharp intensity cutoff for all the acceptor-exciton complexes studied. This is clearly shown for Cd (Fig. 5), Be (Fig. 6), and X (Fig. 10). This effect is obscured by the heavy over-exposure of the $(^{LA}_{1})$ components for Zn (Fig. 3), Mg (Fig. 7), and C (Fig. 8), but can be clearly seen in the $(^{2LA}_{1})$ replica for these acceptors. This shape arises from the facts that $(dE/dk)_{LA}$ remains significant very close to $\vec{k}_x$,[14] and that an appreciable fraction of MC phonon-assisted transitions involve phonons with $\vec{k}_{phon}$ significantly less than $\vec{k}_x$, a result of the finite spread of the wave functions of even weakly bound electrons and holes away from $\vec{k}_x$ and $\vec{k}_\Gamma$. This effect introduces much smaller breadth and negligible asymmetry into the TA-, TO-, and LO-MC replicas, where the corresponding phonon dispersion curves are substantially flat over the outer ~25% of the reduced zone along ⟨100⟩ axes.[14] Of course, curvature of the phonon dispersion curves across the face of the reduced zone at X may also be important for the asymmetry of the LA replica. Very similar phonon replication is seen in the luminescence of excitons bound to Ga-site donors in GaP.[5] The spectra of excitons bound to P-site donors[3] differ fundamentally in the great relative strength of the no-phonon components and of components whose transition matrix element is directly derived from them. These associated components include long-wavelength optical phonon replicas[3] and "two-electron" transitions.[21]

The arrows Zn_R^{LA} and Zn_R^{TO} in Fig. 3 mark the anticipated position for a LA or TO phonon-assisted

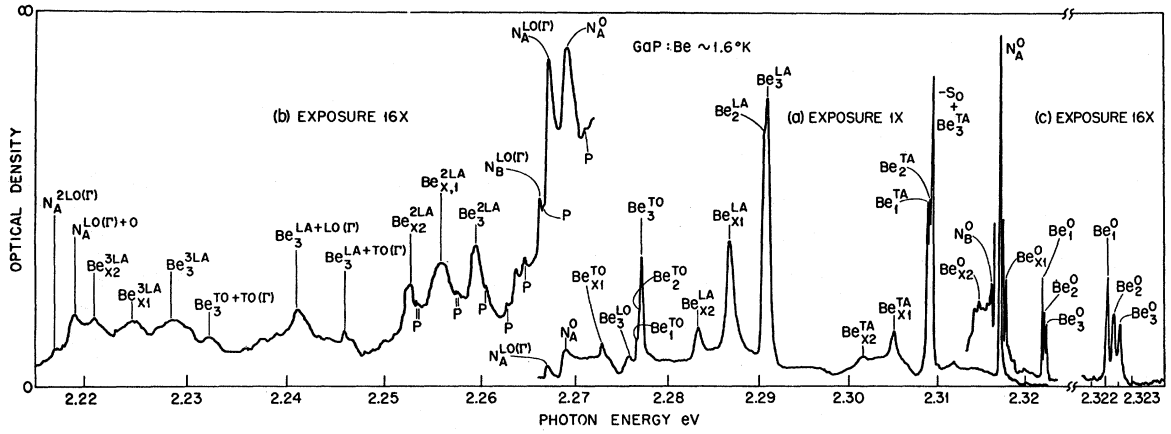

FIG. 6. Low-temperature photoluminescence spectrum of excitons bound to neutral Be acceptors, recorded photographically from a Be-diffused vapor-grown needle. Notation as in Fig. 3. Section (c) shows the no-phonon components on an expanded energy scale.

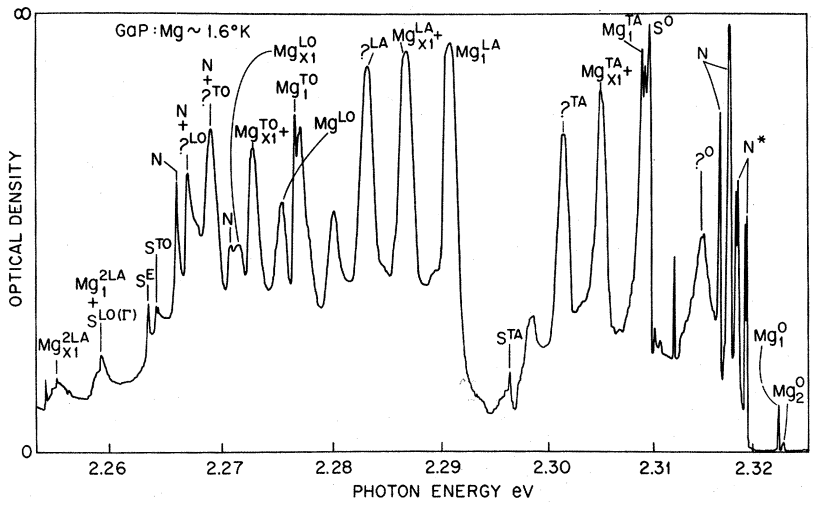

FIG. 7. Low-temperature photoluminescence spectrum of excitons bound to neutral Mg acceptors in GaP, recorded photographically from a solution-grown crystal. Notation as in Fig. 3; the unlabeled weak sharp lines are due to luminescence at distant S-Mg donor-acceptor pairs.

two-hole transition in which the Zn acceptor is left in the 33.3-meV excited state which is prominent in Raman scattering.[22] There is a weak component at this energy in Fig. 3, possibly of this origin. Unfortunately, we were unable to obtain exciton spectra of sufficient quality to confirm the presence of this weak transition for other acceptors. For example, the corresponding component for Be should fall close to the double pair line shown just below Be_3^{2LA} in Fig. 6 according to the systematics of the excitation energy established from Raman scattering by the acceptors Zn, Mg,[22] and C.[23] This Raman transition has not been observed for Cd, the other acceptor for which we could obtain relatively clean exciton spectra (Fig. 5). Again using the established systematics we would predict that this component should fall uncomfortably close to the strong 2LA replica for the Cd exciton.

Most of the acceptor-exciton spectra do not show additional evidence of "two-hole" transitions. As discussed elsewhere,[5] the probability of these transitions is expected to be very small except as sidebands of the no-phonon transitions. Unfortunately, except for Cd, the no-phonon components in the acceptor-exciton spectra are so weak as to prelude the possibility of detecting satellites of them having only a few percent relative intensity against a background of relatively strong components due to multiphonon-assisted exciton decay. However, the Cd-exciton no-phonon line is relatively strong (Table III). Component Cd_1^{2H} in Fig. 5 may be due to a two-hole transition. This component has no analog in the spectra of the much shallower acceptors Zn (Fig. 3) and Be (Fig. 6), and would represent an interbound-state excitation energy of 82.5 meV for the Cd acceptor, corresponding to an excited-state binding energy of 13 meV.[10] This is quite plausible for a nearly effective-mass-like excited state, since

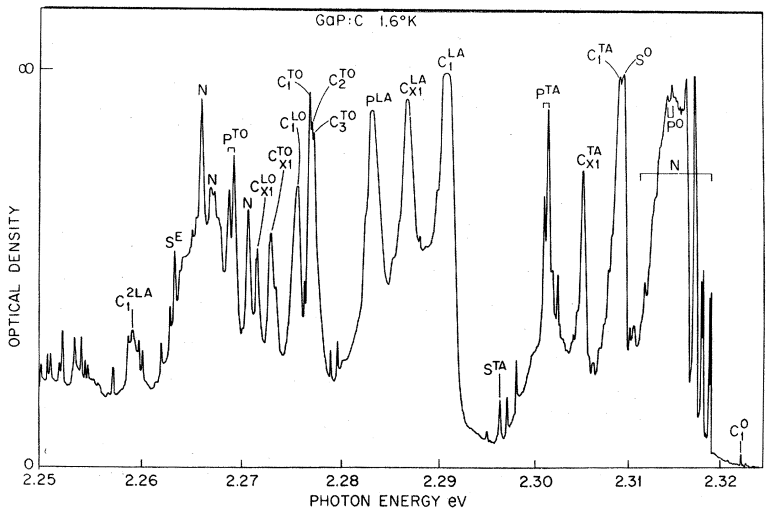

FIG. 8. Low-temperature photoluminescence spectrum of excitons bound to neutral C acceptors in GaP, recorded photographically from a solution-grown crystal. Notation as in Fig. 3; components P^0, etc., are due to residual Si donors. Unlabeled weak sharp lines are due to luminescence at distant S-C donor-acceptor pairs.

the effective-mass ground-state ionization energy is estimated to be 40–45 meV for acceptors in GaP.[10] If this component, or component Zn_R^{LA} discussed above (Fig. 3), *is* due to two-hole recombinations, this would be the first published example of this transition.

The relative strengths of the components in the acceptor-exciton spectra are analyzed in Table III. Ratios for the LO-MC phonon replica are not included in Table III, but it was observed that the TO/LO intensity ratio was ~1.5, independent of the acceptor. Since the LO replica is ~5 times broader than TO, it is appreciably harder to observe and was not recognized amidst strong $k=0$ phonon replicas in an early paper on donor-exciton complexes in GaP.[3] Two reasons for the weakness of the no-phonon components in the acceptor-exciton spectra have been given in Sec. I. Table III shows that these factors indeed account for much of the quantitative differences in the ratios I_{MC}/I_0 between the acceptor and P-site donor-exciton spectra. These ratios are very similar for a Ga-site donor such as Sn and an acceptor complex of nearly equal exciton localization energy, such as Cd. This is consistent with expectation, since the electrons bound in both these complexes should be quasi-p-like, and no-phonon recombinations involving electron scattering through a virtual state derived from the energetically favored Γ_1 conduction-band minimum are forbidden.[24] However, the experimental intensities of the no-phonon transitions decrease with decreasing E_A much more rapidly than accounted for by the effective-mass theory used in Table III. The ratio I_0/I_{MC} increases approximately exponentially with increase in E_{BX} for these point defect acceptors in GaP (Fig. 9), in contrast to the approximately linear variation observed for donors and acceptors in Si at small E_{BX}.[25]

Luminescence due to the decay of excitons at an unidentified shallow neutral acceptor, called X (Fig. 10), has also been reported. This acceptor has axial symmetry.[11] The j-j coupling scheme and magneto-optical properties of this exciton have been discussed elsewhere.[11] Here, we are concerned only to contrast the satellite spectra of this exciton with those of excitons bound to point defects. The position of the lowest no-phonon component X_1^0 deviates but slightly (Fig. 4) from expectation according to the binding energy determined for this axial acceptor.[11] However, Fig. 9 and Table III show that the ratio I_0/I_{MC} is remarkably large for such a low value of E_{BX} (~5 meV), judging by ex-

TABLE III. Parameters of absorption and luminescence of excitons bound to some neutral donors and acceptors in GaP.

Impurity	Ionization energy (meV)	$L_{TA/I0}$[a]	I_{LA/I_0}[a]	I_{TO/I_0}[a]	$(I_{LA/I_0})_{calc}$[b]	$(I_{LA/I_0})_{calc}$[c]
Sulphur (*D*)	104.0	0.009(*L*) 0.011(*A*)	0.015(*L*) 0.02 (*A*)	0.005(*L*) ~0.005(*A*)		0.080(*L*, *A*)
Selenium (*D*)	102.0	0.050(*L*) 0.053(*A*)	0.084(*L*) 0.083(*A*)	0.03 (*L*)	0.016(*L*) 0.021(*A*)	
Tellurium (*D*)	89.5	0.021(*L*) 0.02 (*A*)	0.13 (*L*) 0.03 (*A*)	0.005(*L*)	0.022(*L*) 0.029(*A*)	0.12 (*L*, *A*)
Tin (*D*)	65.5	2.3 (*L*)	5.5 (*L*)	1.1 (*L*)	1.0 (*L*) 1.3 (*A*)	5.3 (*L*, *A*)
X (*A*)	46	1.7 (*L*)	5.1 (*L*)	0.9 (*L*)	2.4 (*L*) 3.2 (*A*)	13 (*L*, *A*)
Carbon (*A*)	48.0	54 (*L*)	250 (*L*)	25 (*L*)	2.2 (*L*) 2.9 (*A*)	12 (*L*, *A*)
Beryllium (*A*)	50	16 (*L*)	40 (*L*)	6.5 (*L*)	2.0 (*L*) 2.6 (*A*)	11 (*L*, *A*)
Magnesium (*A*)	53.5	13 (*L*)	40 (*L*)	~5 (*L*)	1.7 (*L*) 2.2 (*A*)	8.8 (*L*, *A*)
Zinc (*A*)	64.0	22 (*L*) 26 (*A*)	54 (*L*) 88 (*A*)	12 (*L*)	1.1 (*L*) 1.4 (*A*)	5.6 (*L*, *A*)
Cadmium (*A*)	96.5	1.1 (*L*) 2.2 (*A*)	1.8 (*L*) 4.7 (*A*)	0.51(*L*)	0.38 (*L*) 0.5 (*A*)	2.0 (*L*, *A*)

[a]The I_s are integrated intensities for the no-phonon (subscript 0) and MC phonon replicas, measured in luminescence (*L*) and absorption (*A*).

[b]Calculated using the relation $(f_0)_{A,D}=\frac{1}{21}[E_{A,D}/(E_D)_S]^{5/2}\times(f_0)_S$ —Eq. (2) of Ref. 5.

[c]Calculated using the relation $(f_0)_{A,D}=\frac{1}{21}[E_{A,D}/(E_D)_{Se}]^{5/2}\times(f_0)_{Se}$. (The prefactor $\frac{1}{21}$ is omitted in the intercomparison of excitons bound to P-site donors.)

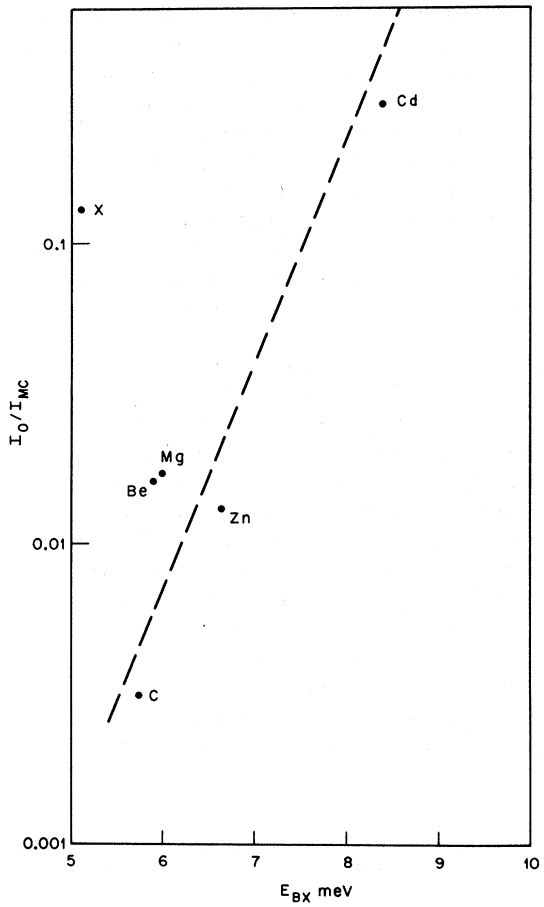

FIG. 9. Dependence on the exciton localization energy of the intensity ratio between the no-phonon component (I_0) and the associated MC replicas (I_{MC}) for the luminescence of excitons bound to neutral acceptors in GaP.

pectation from the experimental trend for the point defect acceptors. Perhaps fortuitously, the observed ratio I_{LA}/I_0 for the acceptor X is close to the value predicted from the donor-exciton spectra. Such large no-phonon oscillator strength indicates strong hole-defect interaction, which is also a prerequisite for the nearly complete quenching of the orbital contribution to the hole g value noted for this acceptor.[11] The main features of the multiphonon spectrum for the X exciton, not shown in Fig. 10, are identical with those shown in Figs. 3, 5, and 6.

No evidence for two-hole transitions to excited states ~35 meV above the ~46-meV-deep ground state of the X acceptor is present in Fig. 10. Such transitions would produce relatively weak satellites near components X_x^{LA}. The origin of these latter components is an intriguing mystery. Clearly, they belong to a series of MC phonon replicas; the corresponding components due to TA and TO phonon-assisted transitions are clearly shown in Fig. 10. The displacement energies below X_1^0 of the two no-phonon spectrum lines deduced from these MC replicas are given in Table I. These satellite lines definitely form part of the luminescence spectrum of the X exciton. Similar satellites displaced a few meV from the principal components are also observed for the Zn, Be, Mg, and C excitons (Figs. 3, 6–8, and Table I). No such satellites were found for the Cd exciton, however (Fig. 5). These satellite spectra all have extremely weak no-phonon components, which are not always observable since they fall close to the no-phonon lines due to residual N. The component Mg_{X1}^0 can be clearly seen in the original photographic spectra from the best crystals, since it falls in the gap between the two groups of N* lines (Fig. 7). The similarity between the C-, Be-, Mg-, and Zn-exciton satellites extends to a near identity of their energy displacements below the principal exciton lines (Table I).

The two general possible models to account for such satellites are (a) interaction with low-energy phonons and (b) two-hole transitions which leave the acceptors in very shallow excited states. Model (b) seems most improbable. States lying ~$E_A/10$ above the acceptor ground state, with precise excitation energies only weakly dependent on E_A, are entirely unanticipated for unstrained GaP crystals. In addition, these satellites exhibit no striking behavior in a magnetic field additional to that exhibited by the principal components. Considering

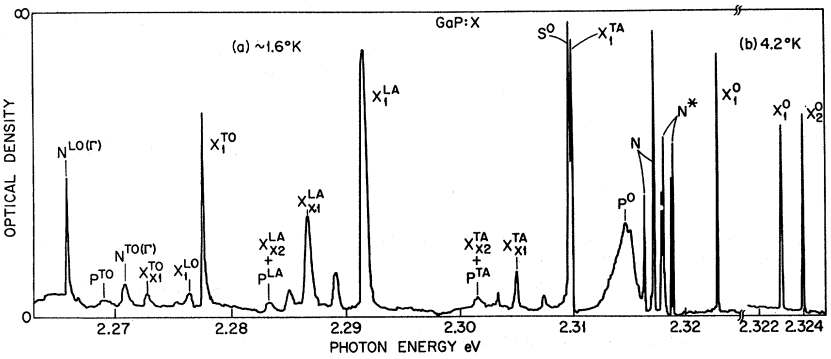

FIG. 10. Low-temperature photoluminescence of excitons bound to neutral X acceptors in GaP, an unidentified complex acceptor, recorded photographically. Notation as in Fig. 3.

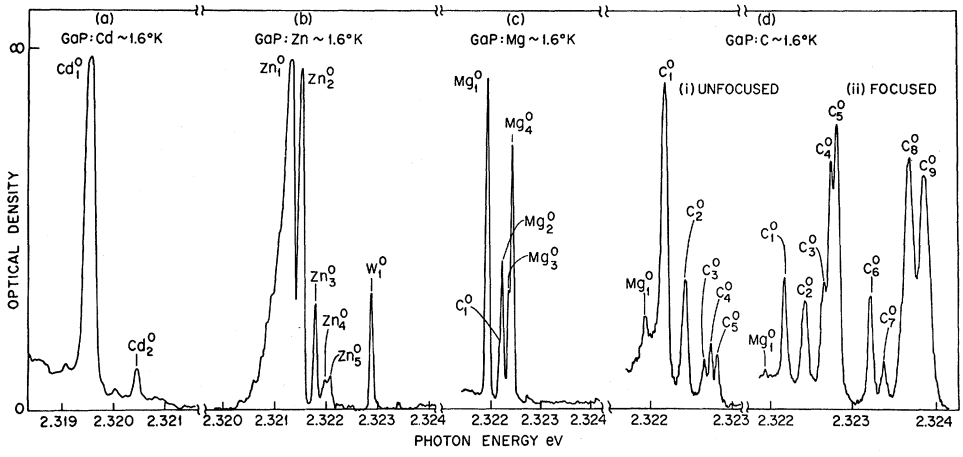

FIG. 11. Details of the zero-field no-phonon lines in the low-temperature photoluminescence of excitons bound to the neutral acceptors Cd, Zn, Mg, and C in GaP, recorded photographically. The effective sample temperature was increased between (d), (i), and (ii) to populate the high initial states of the C-exciton transition, thus enhancing the corresponding luminescence components. The no-phonon lines of the Be exciton are shown in Fig. 6.

model (a), it is clear that the low-energy phonons are not normal in-band resonance modes, since their energies are sensitive neither to the mass defect nor to the lattice site of the acceptor ion. However, the energies in Table I are consistent with acoustical phonons in GaP, [14] strongly coupled for wavelengths comparable to the ground-state radius of the neutral acceptor. Morgan has suggested[26] that these may be T_2 modes which can control the properties of bound holes in a zinc-blende semiconductor such as GaP through the dynamic John-Teller effect.[27] The principal structure in these satellite spectra (Table I) might be vibronic, while the substructure clearly resolved for the Zn acceptor (Fig. 3) might be rotational. This seems to be the only plausible model for these components, although their absence in the Cd-exciton spectrum (Fig. 5) remains unexplained.

B. *J-J* Coupling and Magneto-Optics

Unlike excitons bound to neutral *P*-site donors, the acceptor-exciton complexes in GaP all contain several no-phonon lines (Fig. 11). This structure does not arise from excited orbital states of the bound particles, and many of the no-phonon lines in the acceptor-exciton spectra have comparable oscillator strengths (Table IV). This complexity of the acceptor-exciton spectra has several causes (Fig. 12). First, two $j=\frac{3}{2}$ holes may combine to form two states, $J=0$ and $J=2$ [Fig. 12(a)]. By contrast, only one state ($J=0$) is allowed for two $s=\frac{1}{2}$ electrons bound to a *P*-site donor. Next, the electron is repelled by the acceptor core, and therefore will not experience a large valley-orbit splitting. For acceptors which are point defects on the Ga site, in fact, the electron valley-orbit state will be a "pseudo"-*p*-state transforming as Γ_5 under the T_d point group [Fig. 12(b)].[5,24] The Γ_8 state is shown lowest in Fig. 12(b), to illustrate the simplest situation where, preserving *small* crystal field splittings, the lowest-energy exciton transition may be a Kramers doublet with a small initial-state g factor, in agreement with experiment for the Cd and Zn excitons (see below). By contrast, electrons bound to attractive *P*-site donors have *s*-like wave functions, transforming as Γ_1. Combining these effects, Fig. 12(c) shows that a total of 12 no-phonon lines might be seen in zero magnetic field.

Nine of these lines may have been seen at high excitation intensity for the shallow acceptor C in Fig. 11(d), where the zero-field separations are minimal. However, no definitive assignment of these weak lines can be made, since it was impossible to resolve clearly the magnetic behavior of other than the lowest-energy lines associated with the deepest acceptors (see below). It is therefore possible that some of the lines in Fig. 11(d) are connected with states additional to those considered in Fig. 12(c), although it is certain that they all belong to the C exciton.

TABLE IV. Relative oscillator strengths of zero-field no-phonon components of acceptor excitons in GaP.

Acceptor	$f\binom{0}{2}$[a]	$f\binom{0}{3}$[a]	$f\binom{0}{4}$[a]	$f\binom{0}{5}$[a]
X	20	•••		
Mg	1.0	4[b]		
Cd	0.2_8	0.9_2	0.7	0.7

[a]Assuming $f\binom{0}{2}=1.0$.

[b]Probably more than one component (unresolved).

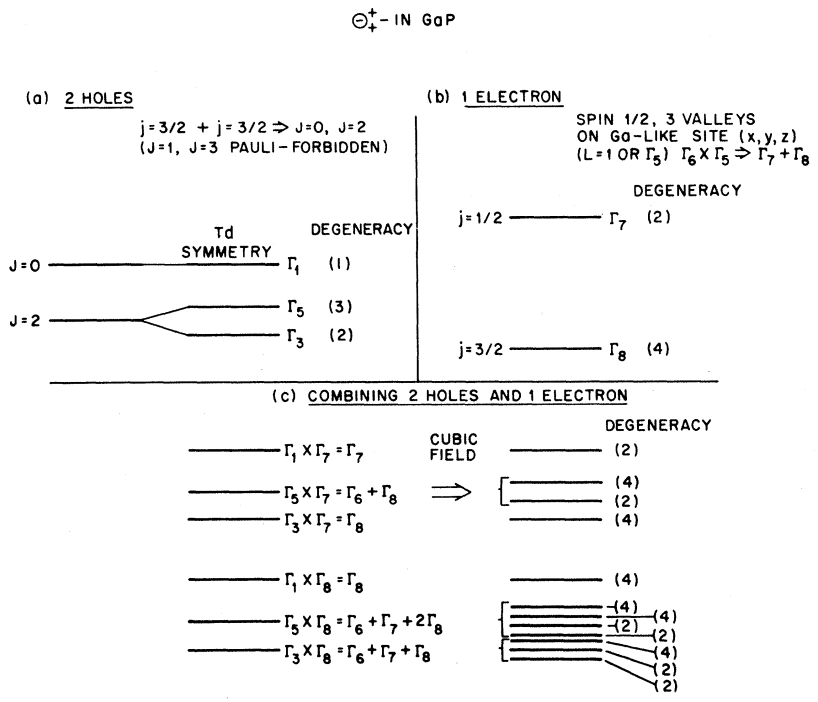

FIG. 12. $J-J$ coupling scheme and the group theory of excitons bound to neutral point defect substitutional acceptors in GaP. Part (a) shows the states formed by coupling two $j=\frac{3}{2}$ holes, part (b) the states of an electron bound to a Ga-like (nonattractive) site, including spin-orbit coupling, and part (c) illustrates the combination of these states. The energy ordering in (a) is consistent with Ref. 27, that in (b) is discussed in the text. The relative splittings are purely schematic, and in (c) the *ordering* of closely spaced levels is also schematic.

The total degeneracy of the states shown in Fig. 12(c), in principle capable of being lifted in a magnetic field, is 36. In addition, the final state of the exciton transition splits into four. Thus, the total possible number of Zeeman transitions is 144, the majority of which are allowed. The final state of the transition is a simple hole bound to a T_d symmetry acceptor, and no zero-field splittings can occur. Thus, all the higher-energy zero-field subcomponents are subject to thermalization in luminescence and are very weak at the lowest temperatures. These zero-field splittings increase with the localization energy E_{BX} of the lowest line, and only one higher-energy component can be seen for the deepest acceptor Cd [Fig. 11(a)]. The no-phonon lines are too weak to be significant in absorption for the shallowest acceptors. Even for the deeper acceptors, acceptor-exciton absorption can only be seen at high impurity concentrations, where the detailed no-phonon structure cannot be resolved (Sec. III C).

As is usual for bound excitons in semiconductors, studies of the Zeeman effect provide important evidence of the nature of the centers to which the excitons are bound. Of the acceptor excitons in GaP, that due to Cd is the easiest to study, both because the no-phonon line intensity is by far the strongest (Table III) and because the splitting between the zero-field lines [Fig. 11(a)] is larger than the magnetic splittings, so that interactions between magnetic subcomponents from different initial states are minimized.

The basic Zeeman pattern for the Cd_1^0 no-phonon line shown in Fig. 13 can be interpreted on the simple energy-level scheme given in the insert.

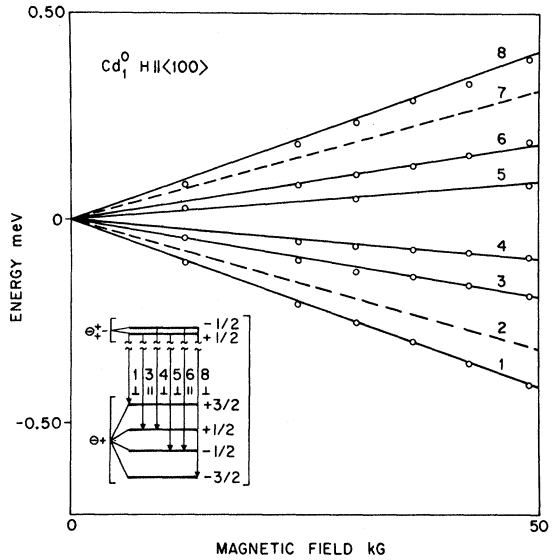

FIG. 13. Zeeman splitting of the lowest (Cd_1^0) no-phonon line observed in the luminescence of the Cd exciton as a function of H for $H\parallel(100)$. The dashed lines represent forbidden transitions. Points are experimental, lines are theoretical. The inset shows the magnetic substates of the Cd exciton θ_+^+ and neutral Cd acceptor $\theta+$, the allowed transitions between them for electric dipole radiation, and their polarization.

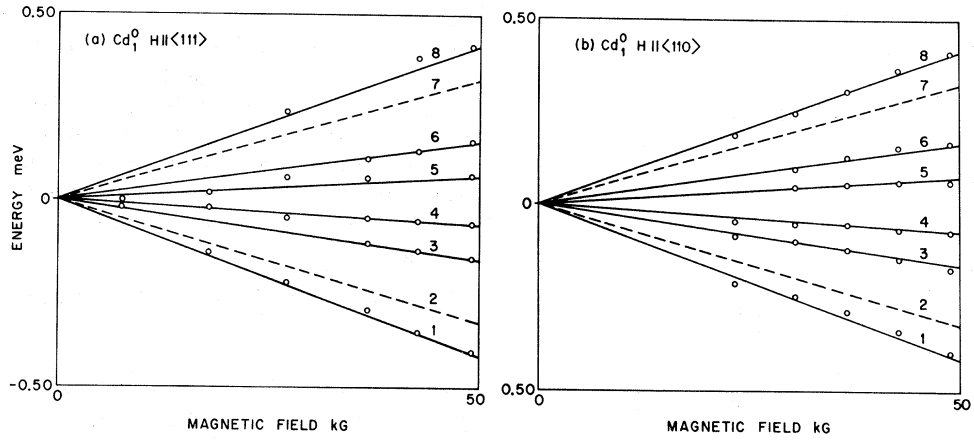

FIG. 14. Zeeman splittings of the Cd_1^0 no-phonon luminescence line as a function of H, (a) for $H \parallel \langle 111 \rangle$ and (b) for $H \parallel \langle 110 \rangle$. The notation corresponds to Fig. 13.

A gross splitting into four with additional fine splitting resulting in a doubling of each of these four lines can be recognized immediately. Components exhibiting the gross splitting show no evidence of thermalization of relative intensity, even when $(\Delta E)_H \sim 6kT$ (1.6 °K and 50 kG). This gross splitting is therefore assigned to the final state of the luminescence transition. However, slight thermalization is observed between lines 4 and 3, between 6 and 5, and between 8 and 1, $(\Delta E)_H \sim 2kT$, supporting the level scheme shown.

The four magnetic components of the final state are those of a simple $J = \frac{3}{2}$ acceptor on a T_d lattice site. Consider the model Zeeman Hamiltonians[28]:

$$H^{(2)} = g_{\mathrm{eff}}\, \mu_B \vec{S} \cdot \vec{H}$$
$$= \mu_B [K \vec{J} \cdot \vec{H} + L (J_x^3 H_x + J_y^3 H_y + J_z^3 H_z)] \qquad (3)$$

for the initial and final states, where $S = \frac{1}{2}$, $J = \frac{3}{2}$, and μ_B is the Bohr magneton. We then find from Cd_1^0 that

$$g_{\mathrm{eff}} = -0.32 \pm 0.04, \quad K = 0.99 \pm 0.04, \quad L = 0.07 \pm 0.02. \qquad (4)$$

The value for K is similar to that observed for other relatively weakly bound holes in GaP.[29,30] This result for the anisotropy parameter L, together with previous work in GaP, e.g., Table III of Ref. 5, suggests that L is small and positive for very weak binding (i.e., for free holes), but becomes negative for the deeper states, with $-L$ increasing with the hole localization energy. The g values in Eq. (4) above were determined by considering Zeeman data for $H \parallel \langle 111 \rangle$ and $H \parallel \langle 110 \rangle$ also (Fig. 14). The weak outer components 1 and 8 and the small splittings $h\nu_6$-$h\nu_5$ and $h\nu_4$-$h\nu_3$ were hard to resolve below ~ 20 kG. The effect of the anisotropy parameter L is more clearly seen in Fig. 15, which shows theoretical data at $H = 50$ kG obtained with the parameters given in Eq. (4).

The complication inherent in the initial state of the acceptor-exciton transition in a multiconduction-band semiconductor such as GaP has already been emphasized (Fig. 12). However, for Cd_1^0 we have a single initial state split far below the many other states possible in zero field [Fig. 11(a)]. The Zeeman study shows that this initial state splits simply into two, with a small isotropic g factor. This behavior and the magnitude of g_{eff} suggests that this lowest initial state is Γ_6, and Fig. 12(c) has been drawn with this feature in mind. A g factor of $-\frac{1}{3}$ is consistent with expectation if the initial-state degeneracy has been lifted to the maximum extent possible in the cubic crystal field of the GaP lattice. The experimental evidence for the

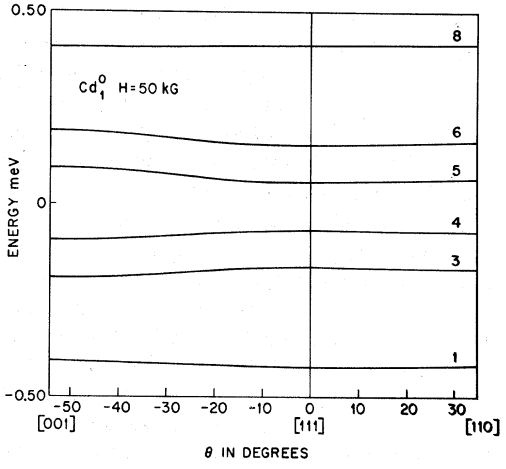

FIG. 15. Zeeman splittings of the Cd_1^0 no-phonon luminescence line calculated as a function of the angle of H in a ⟨110⟩ plane from a fit to the experimental data in Figs. 13 and 14.

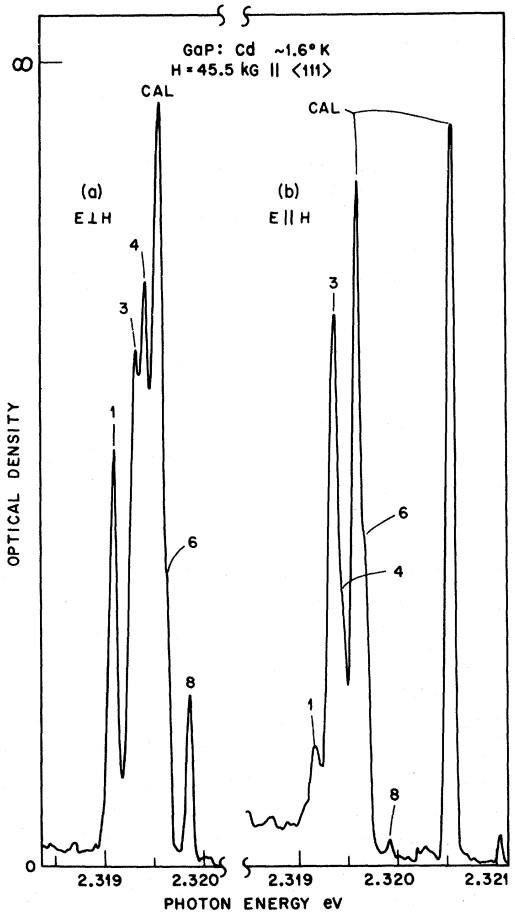

FIG. 16. Zeeman pattern of the the Cd_1^0 no-phonon line recorded photographically for $H = 45.5$ kG $\parallel \langle 111 \rangle$, (a) for $E \perp H$ and (b) for $E \parallel H$. The notation corresponds to Fig. 13. Line 5 is obscured by the Ne calibration line.

(negative) sign of this initial-state splitting is twofold. First, as is shown in Figs. 13 and 14, transitions labeled 2 and 7 are not detected. These transitions are forbidden by electric dipole selection rules ($\Delta m_j = 2$), according to the insert in Fig. 13, provided the $m_j = +\frac{1}{2}$ initial state lies lowest. Subcomponents 1 and 8, exhibiting the maximum magnetic splitting, would be forbidden if the $m_j = -\frac{1}{2}$ initial state lay lowest. This assignment of g_{eff} is also consistent with the polarization data in Fig. 16. Magnetic subcomponents 1, 4, and 8 are much stronger for $E \perp H$, whereas 3 and 6 are relatively strong for $E \parallel H$. Subcomponent 5 is obscured by the Ne calibration line at 2.319 59 eV. If the sign of g_{eff} was reversed, Fig. 13 insert shows that the polarization properties within the pairs of subcomponents 3, 4 and 5, 6 would reverse and become inconsistent with Fig. 16.

Additional quantitative Zeeman data were taken only for the Zn exciton. Here, problems arise from the fact that the relative strength of the Zn_1^0 no-phonon line is much less (Table III) and the zero-field splitting $\Delta E(Zn_2^0 - Zn_1^0)$ is only 0.22 meV, comparable with the magnetic splittings at fields adequate to resolve the magnetic subcomponents clearly (Fig. 17). Satisfactory data were obtained only for $H \parallel \langle 111 \rangle$, using a vapor-grown needle with a $\langle 111 \rangle$ growth axis. In Fig. 17 the magnetic splitting of Zn_1^0 is fitted to Eq. (3) with the following parameters:

$$g_{eff} = \text{unresolved}, \qquad K = 0.99 \pm 0.05, \qquad L = 0.0 \pm 0.03. \tag{5}$$

These hole g values are consistent with the above remarks in that $|L|_{Zn} < |L|_{Cd}$, since the acceptor Zn is significantly shallower than Cd. We were not able to resolve the small minimal initial-state splitting $|g_{eff}| \sim \frac{1}{3}$, expected from the analysis in Fig. 12. Unfortunately, the magnetic subcomponents for the shallow Zn exciton were not as sharp as for the deepest Cd exciton in our best crystals. At the high fields >40 kG needed to overcome this disadvantage, there is considerable interaction between subcomponents from Zn_1^0, Zn_2^0, and even higher zero-field transitions, as is clearly seen in Fig. 17. This is believed responsible for our failure to resolve the fine splitting of the lines 3, 4 and 5, 6 expected from the minimal g value ($\frac{1}{3}$) predicted for the Γ_6 subcomponents of the initial state. These problems are appreciably worse for the shallower excitons Mg, Be, and C, where the zero-field energy splittings are even smaller (Figs. 6 and 11).

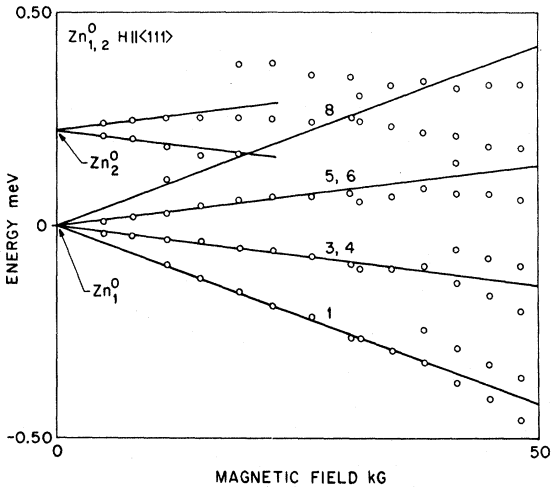

FIG. 17. Zeeman splittings of the $ZN_{1,2}^0$ no-phonon lines as a function of H for $H \parallel \langle 111 \rangle$. Not all of the magnetic subcomponents were resolved, especially for Zn_2^0, and some points appear above ~20kG from still higher-energy zero-field lines. Nonlinearity above ~35 kG is due to interactions between transitions from Zn_1^0 and Zn_2^0, but the data are insufficiently clear for this interaction to be assessed quantitatively.

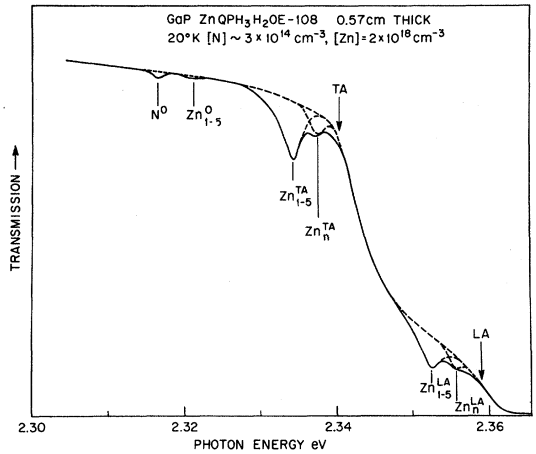

FIG. 18. Portion of the transmission spectrum of a heavily Zn-doped GaP vapor-grown needle containing broad lines attributed to the combined effects of lines $Zn_1^0 \rightarrow Zn_5^0$ shown in Fig. 11(b), which have uniform oscillator strength (Table IV), and their TA- and LA-MC phonon replicas. Components subscript n are discussed in the text. The underlying absorption represented by the upper dashed lines and their smooth interpolation is intrinsic.

However, it was established that the gross splittings of Mg_1^0 and Be_1^0 at low fields were similar to Fig. 17, confirming the presence of a single hole in the *final* state of these transitions also, since no thermalization occurs for these magnetic subcomponents.

C. Absorption Spectra of Neutral Acceptors and the Radiative Lifetime of Bound Excitons

The small no-phonon oscillator strength of the acceptor-exciton transitions makes it impossible to record absorption spectra by conventional means in crystals sufficiently lightly doped that the detailed structure can be seen. Figure 18 shows the broadened exciton absorption recorded from a 5.7-mm GaP needle doped with 2×10^{18}-cm^{-3} neutral Zn acceptors. The principal components are due to TA- and LA-MC phonon-assisted transitions, consistent with expectation from Fig. 3 assuming mirror symmetry of the phonon replicas in the no-phonon line. Table III shows that the relative strengths of these phonon replicas in the absorption and luminescence spectra are quantitatively mutually consistent.

Two broad lines are clearly resolved in the TA and LA phonon-assisted Zn-induced absorption in Fig. 18. These lines are superimposed upon intrinsic absorption due to the photocreation of free excitons with the emission of MC-TA and -LA phonons. The fine structure observable near the thresholds of these square-root absorption thresholds in undoped refined GaP[31] cannot be resolved from this crystal. The energies of the lower-energy absorption components Zn_{1-5}^{TA} and Zn_{1-5}^{LA} correspond to a no-phonon component Zn_{1-5}^0 just below 2.322 eV, near the centroid of the group of five no-phonon lines observed in luminescence (Fig. 11), which we have seen have comparable oscillator strengths (Table IV). The higher-energy broad components Zn_n^{TA} and Zn_n^{LA} lie 3.0 meV above components Zn_{1-5}^{TA} and Zn_{1-5}^{LA}, and the corresponding no-phonon component Zn_n^0 is too weak to be clearly distinguished. It might be thought that component Zn_n^0 contains the higher-energy group of no-phonon lines expected from the j-j coupling model of this complex [Fig. 12(c)]. However, this group of lines should lie close to the strong components $C_{8,9}^0$ shown in Fig. 11, if their position is little affected by central-cell interactions. In fact, Zn_n^0 lies about 1 meV *higher* than $C_{8,9}^0$.

For a Gaussian broadened line, neglecting local-field corrections for very diffuse bound-exciton states, the oscillator strength is given by

$$f = 9.6\times10^{15} n\, \alpha_{max}\, \Gamma/N\ . \qquad (6)$$

In Eq. (6), n is the refractive index and N is the concentration of optically active centers (neutral Zn acceptors). The absorption cross section $\alpha_{max}\Gamma$ of the components Zn_{1-5}^0, + Zn_{1-5}^{TA} + Zn_{1-5}^{LA} is 4.2×10^{-3} cm^{-1} eV. The total absorption cross section for this transition is $\sim 4.8\times10^{-3}$ cm^{-1} eV, allowing for the TO component by using the relative strengths determined from luminescence (Table III). Hall-effect measurements indicate that $(N_A-N_D) = 2.1\times10^{18}$ cm^{-3} for this sample in the dark. Control experiments showed that this large value of (N_A-N_D) was not significantly altered by optical pumping at the light levels used in the absorption measurements. Using these experimental parameters, with $n = 3.47$, Eq. (6) gives $f = 7.8\times10^{-5}$ for this vapor-grown needle. Measurements on other crystals gave slightly differing results and a reasonable average is $f = 6\pm2\times10^{-5}$. We take this to represent absorption at five equally weighted no-phonon components (Table IV), and hence conclude that $f_1 = 1.2\times10^{-5}$ for the lowest-energy component of the Zn exciton. Assuming detailed balance, the radiative lifetime τ_R is

$$\tau_R^{-1} = (nf/1.5\lambda^2)(g_1/g_2)\ , \qquad (7)$$

where λ is the transition wavelength and g_2, g_1 are the degeneracies of the initial and final states of the luminescence transition, respectively, 2 and 4 according to Fig. 13 inset. From Eq. (7), $\tau_R = 55$ μsec for the Zn_1 transition.

We were unable to make satisfactory electrical plus optical measurements to determine f, and hence τ_R, for the other acceptors, mainly because it was not possible to obtain sufficiently high concentrations of the desired dopant with sufficiently low concentrations of inadvertent dopants, espe-

cially N. Absorption of the Cd exciton was also seen from vapor-grown needles (Table III), but the appropriate values of N_A-N_D were uncertain because of optical pumping in the absorption experiment. However, we can conclude that τ_R should be similar for exciton recombination over the whole range of acceptors contained in Table III, since the fractional oscillator strength in the no-phonon transition increases the transition rate by only ~30% for the acceptor Cd and by a much smaller amount for the other acceptors.

We may compare the Zn-acceptor oscillator strength with that previously reported for S donors by anticipating that $f_{Zn} = f_S \times \Delta$, where Δ is the fractional oscillator strength in the TA + LA + TO phonon replicas of the S exciton (3.6%[3]). Using the oscillator strength quoted in Ref. 3, corrected for a factor of $\frac{1}{9}$ omitted from the right-hand side of Eq. (4) in that paper, we predict $f_{Zn} = 3 \times 10^{-5}$, about 2.5 times the observed value. Much better agreement with the experimental value of f_{Zn} is obtained using Pikhtin and Yas'kov's[32] absorption cross section for S, which is ~30% of the value quoted in Ref. 3.

The experimental lifetimes of the acceptor-exciton luminescence were determined using the system shown in Fig. 2. The sampling scope recording channel was appropriate for these short lifetimes. The Dumont 150 UVP photomultiplier was terminated with 50 Ω. Sample temperatures were $\lesssim 1.65$ °K throughout, so that the luminescence measured was predominantly due to the lowest-energy component of each set of exciton transitions. The spectrograph setting was adjusted so that only appropriate light was detected by the photomultiplier; usually the strong LA-MC replica was selected. For the Cd and X excitons, decay-time measurements were also made on the relatively intense no-phonon components. The time decays were generally exponential over better than a decade, although a poor signal-to-noise ratio prevented a very close check of this for the C acceptor.

The experimental lifetimes τ_E are compared in Table V with the values predicted for radiative decay. The ratios τ_R/τ_E are all $\gg 1$, ~500 for the Zn exciton (Table V). A similar discrepancy has been explained for exciton recombination of neutral donors in GaP and Si[7] by postulating that τ_E is determined by a nonradiative Auger decay channel, in which the whole of the transition energy appears as kinetic energy of the second electron which is ejected deep into the conduction band. The hypothesis is consistent with the low radiative efficiency of this recombination process.

TABLE V. Branching ratio $b = \tau_R/\tau_E$ for the recombination of excitons at neutral acceptors in GaP.

Acceptor	τ_R(μsec)[a]	τ_E(nsec)	$b = \tau_R/\tau_E$
X	50	300	170
C	55	280	200
Be	55	•••	•••
Mg	55	190	290
Zn	55	110	500
Cd	42	14	3000

[a]Marginally overestimated, since the satellites in Table III and the multiphonon replicas were disregarded.

Similar nonradiative processes involving the ejection of holes into the valence band of GaP have been inferred from the temperature dependence of the intensity and decay time of the red luminescence in GaP: Zn, O[33] (interaction with free holes), and from the quenching of electron-capture luminescence at the deep O donor by interaction with holes bound to neutral acceptors.[34] However, the observation of the Auger effect for excitons bound to neutral acceptors provides a very direct measure of the branching ratio $b = \tau_R/\tau_E$ between nonradiative and radiative decays for hole ejection.

Table V shows that b is very sensitive to the localization energy of the exciton at the neutral acceptors. This variation is almost entirely due to a sharp dependence of τ_E on E_A. Figure 19 shows that the Auger transition probability P_E varies with E_A approximately according to

$$P_E \propto \frac{1}{\tau_E} \propto E_A^n , \tag{8}$$

where $n \sim 4.5$. This strong variation of P_E has two causes. First, the Auger rate depends upon the overlap in real space between the two like particles (holes) in the exciton complex. In the spirit of the sudden approximation,[5] in which the wave function of one hole comes mainly from the acceptor ground state while the other hole is relatively weakly bound, the hole-hole overlap is primarily determined by $|\Psi_s|^2$ for the shallow hole, evaluated near the acceptor core where the tightly bound hole is confined. For an S state

$$|\Psi|^2_{\text{small } r} \propto E_{Bx}^{3/2} . \tag{9}$$

Momentum must be conserved in the Auger transition. This gives rise to an additional dependence of P_E on E_A. The hole momentum $\vec{k}_f$ in the final state of the Auger transition is very large, corresponding to the large-hole kinetic energy $\epsilon(k) \sim 2.3$ eV. Momentum conservation via interaction between the hole and the acceptor ion depends on $|\Psi_a|^2_{\vec{k}=\vec{k}_f}$ for the tightly bound hole in the initial state, corresponding to a hole binding energy E_A. In the approximation that the valence bands may be represented by a single spherical band with hydrogenic acceptor wave functions,

$$|\Psi_a|^2_{\vec{k}=\vec{k}_f} \propto \frac{E_A^{5/2}}{[E_A + \epsilon(k_f)]^4} \tag{10}$$

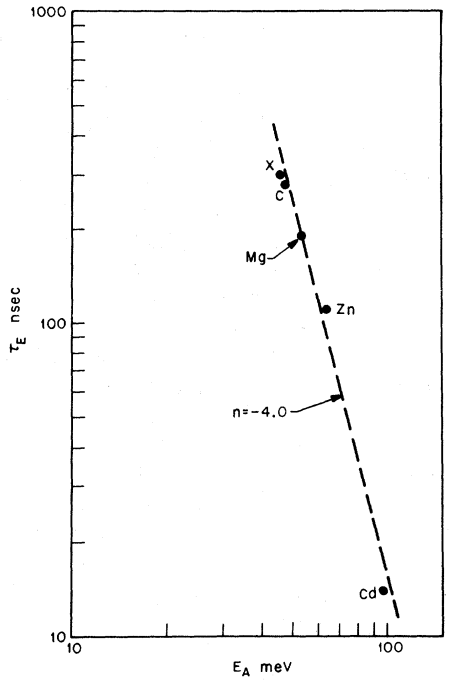

FIG. 19. Dependence on the acceptor ionization energy of the experimental decay time τ_E of excitons bound to the neutral acceptors X, C, Mg, Zn, and Cd. The slope of the dashed line, -4.0, indicates the variation predicted from a simple model with hydrogenic energy states and a single spherical valence band.

is the appropriate asymptotic form, where hole energy is reckoned positive below E_A. For the Auger transitions, $\epsilon(\vec{k}_f) \gg E_A$ and Eq. (10) shows that $|\Psi_a|^2 \propto E_A^{5/2}$. Combining the factors in Eqs. (9) and (10), and noting that changes in E_{BX} are proportional to changes in E_A (Fig. 4), the total dependence of P_E on E_A predicted by this simple theoretical model has the form of Eq. (8), with $n = 4.0$.

The simple model outlined above neglects all details of the valence-band structure; in reality the valence bands are far from spherical, especially at large $\epsilon(k)$. In view of this, the close description of the experimental data in Fig. 19 by this simple theory is remarkable. However, this crude approximation is more realistic for the valence-band structure of GaP than for the conduction-band structure. The calculations of Cohen and Bergstresser[35] suggest that energy can be conserved in the Auger recombination of donor-exciton complexes simply by an interconduction-band transition, unlike the corresponding process for acceptor-exciton complexes. Thus, details imposed on the band structure by the lattice periodicity may be more important for Auger decays at donor-exciton complexes. The donor-exciton Auger rate[5,7] is significantly smaller than for acceptor excitons for comparable values of E_{BX} and E_D or E_A.

The data in Fig. 19 could have significant implications for the fabrication of efficient GaP light-emitting diodes. Extrapolation of Fig. 19 to $E_A = 203$ meV, appropriate for the deep acceptor Si,[8] suggests that τ_E may be as small as 1 nsec for this exciton complex. Figure 4 indicates that $E_{BX} \sim 15$ meV for the Si acceptor, deeper than the radiative bound state due to N.[36] Thus Si, a persistent residual impurity of GaP grown in furnaces with SiO_2 components, produces a moderately deep bound-exciton state with extremely low radiative efficiency and decay time, a model luminescence killer center. Estimates from Table V suggest that the branching ratio in favor of nonradiative decay for the Si-acceptor exciton may be ~ 10 000 if τ_R is 10 times smaller than for Cd because of the assumed predominance of no-phonon transitions in the decay of this relatively deep exciton (extrapolation of Fig. 9 to $E_A = 203$ meV). Attention has already been drawn to the likelihood that strong luminescence quenching may be produced from the decay of excitons bound to the deep neutral donor O.[34] The weak luminescence anticipated for the Si and O excitons has yet to be identified experimentally, but theory leaves no doubt that the relevant bound-exciton states should exist.[4] The shallow Si donor also exhibits a similar value of b for bound exciton decay. However, these Si bound excitons are both relatively shallow. The significance of this nonradiative mechanism may be considerably reduced at 300 °K in GaP doped to the levels typical for light-emitting diodes, because of tunneling and thermal liberation of the bound excitons before nonradiative recombination can occur. Even so, the above considerations suggest that the concentration of Si in GaP grown for device purposes should be reduced to minimal practicable levels.

IV. SUMMARY

The radiative decay of excitons bound to six different shallow acceptors has been identified in GaP, confirming theoretical predictions of the existence of these bound states. Evidence for this identification is obtained from measurements on refined, deliberately doped, crystals, from the magnitude of the exciton localization energy and its dependence on the acceptor ionization energy, and from Zeeman studies of the no-phonon transitions. The hole g values obtained from this study are consistent with previous results for weakly bound holes in GaP. Many no-phonon components are easily seen for the shallower acceptors. For the deepest acceptor Cd, the energy spacing between the lowest-energy exciton states becomes relatively large and the majority of the higher states cannot be populated and seen in luminescence. The multiplicity of no-phonon states occurs because *two* values of combined angular momentum are allowed by the ex-

clusion principle for two $j = \frac{3}{2}$ holes and because of the high degeneracy of an electron bound to a center with a repulsive central cell in GaP. Many of the lowest-energy no-phonon lines have comparable oscillator strengths. These individual no-phonon lines cannot be resolved in absorption, but their collective effect has been seen for the deeper Zn and Cd acceptors. The radiative decay times τ_R of the lowest-energy states of these excitons have been estimated from the absorption cross section measured for the Zn exciton, using information about the intensity ratio between the no-phonon components and the (MC) phonon replicas obtained from the luminescence spectra. The no-phonon components are weak compared with excitons bound to neutral P-site donors, as anticipated. The radiative decay times thus obtained are more than two orders of magnitude longer than the experimental values τ_E, depending on the acceptor. This discrepancy is due to the predominance of a totally nonradiative (Auger) decay channel for these exciton complexes, consistent with expectation for an indirect-gap semiconductor. The dependence of the decay-time discrepancy on the acceptor is mainly due to a strong dependence of τ_E on the acceptor binding energy E_A. Experimentally $\tau_E \propto E_A^{-n}$ where $n \sim 4.5$, remarkably close to the value 4.0 predicted from simple theoretical considerations. This is the first experimental study of the binding-energy transition-rate systematics of Auger recombinations in semiconductors. It is clear from this study that the deepest neutral donors and (particularly in GaP) acceptors are strong luminescence quenching centers for excitons. In particular, these considerations indicate that Si contamination should be avoided in GaP crystals from which light-emitting diodes are made.

After this paper was submitted for publication, a paper describing the absorption and luminescence of excitons bound to neutral C, Zn, and Cd acceptors in GaP was published by Vink and Peters.[37] The luminescence spectra were less well resolved, owing to residual strain in the GaP layers grown by vapor-phase epitaxy, it is claimed, but possibly also owing to inadequately low impurity concentrations in the majority of their crystals. No Zeeman studies were made by Vink and Peters, and they were unable to measure the true decay times of excitons bound to these three acceptors. In addition, the authors attention has been drawn to a report of two-hole transitions in GaAs, recently submitted for publication.[38] The relative oscillator strengths of the no-phonon lines in the GaAs acceptor-exciton spectra are relatively large, and the two-hole spectral components are correspondingly more clearly defined than reported here for GaP.

ACKNOWLEDGMENTS

The authors are grateful to J. J. Hopfield for several enlightening discussions of the properties of bound excitons in GaP. They also thank T. N. Morgan for suggesting a vibronic model for the X satellite series observed for the five shallowest bound excitons. Generous assistance in connection with the acousto-optical modulator was provided by R. L. Hartman and D. A. Sealer. Expert technical assistance was obtained from G. Kaminsky on the spectroscopy and from R. B. Zetterstrom in crystal growth.

---

†Present address: Royal Radar Establishment, Great Malvern, Worcestershire, England.

*Present address: National Institute for Researches in Inorganic Materials, Tokyo, Japan.

[1]P. J. Dean, R. A. Faulkner, and S. Kimura, Solid State Commun. 8, 929 (1970).

[2]D. G. Thomas, M. Gershenzon, and F. A. Trumbore, Phys. Rev. 133, A269 (1964).

[3]P. J. Dean, Phys. Rev. 157, 655 (1967).

[4]J. J. Hopfield, in *Proceedings of the International Conference on the Physics of Semiconductors, Paris*, 1964 (Dunod, Paris, 1964), p. 725.

[5]P. J. Dean, R. A. Faulkner, and S. Kimura, Phys. Rev. B 2, 4062 (1970).

[6]E_{BX} is defined simply as the energy between the no-phonon line of the bound-exciton transition and the energy threshold for free excitons, E_{gx}.

[7]D. F. Nelson, J. D. Cuthbert, P. J. Dean, and D. G. Thomas, Phys. Rev. Letters 17, 1262 (1966).

[8]P. J. Dean, C. J. Frosch, and C. H. Henry, J. Appl. Phys. 39, 5631 (1968).

[9]C. J. Frosch, in *Proceedings of the International Conference on Crystal Growth, Boston*, 1966, edited by H. Steffen Peiser (Pergamon, New York, 1967), p. 305.

[10]P. J. Dean, E. G. Schönherr, and R. B. Zetterstrom, J. Appl. Phys. 41, 3474 (1970).

[11]P. J. Dean, R. A. Faulkner, and E. G. Schönherr, in *Proceedings of the International Conference on Semiconductor Physics, Cambridge*, 1970 (U.S. Atomic Energy Commission, Oak Ridge, 1970), p. 286.

[12]M. Ilegems and W. C. O'Mara, J. Appl. Phys. (to be published).

[13]D. Maydan, IEEE J. Quant. Electron. QE-6, 15 (1970).

[14]All optical properties of shallow bound excitons in GaP studies so far are consistent with the assumption that the conduction band valleys are at X. Comparison of the energies of the MC phonons with the phonon dispersion curves of GaP determined by inelastic neutron scattering [J. L. Yarnell, J. L. Warren, R. G. Wenzel, and P. J. Dean, *Neutron Inelastic Scattering* (International Atomic Energy Agency, Vienna, 1968), p. 301] indicates that the conduction-band minima could lie inside the reduced zone at most only a few percent of $\vec{k}_x$. The shape of the LA-MC phonon replica in these very shallow bound-exciton spectra probably constitutes the best evidence that the conduction-band minima occur *right at* the zone boundary at X.

[15]The so-called P bound-exciton lines, frequently observed in lightly Si-contaminated GaP, have been tentatively attributed to the decay of excitons bound to neutral Si acceptors (Fig. 4 of Ref. 14). However, the point $E_A = 203$ meV, $E_{BX} = 14$ meV falls well below the curve in Fig. 4. For this and other reasons, we now believe that the P lines arise from the decay of excitons bound to neutral Si *donors*. This will be discussed further elsewhere.

[16]J. R. Haynes, Phys. Rev. Letters 4, 361 (1961).

[17]M. A. Lampert, Phys. Rev. Letters 1, 450 (1958).

[18]Further evidence on this point will form the subject of a separate publication.

[19]Considerable difficulties were experienced in obtaining clean Mg-exciton spectra which exhibited the associated low-energy structure clearly, because of C contamination. We have seen that both C and Mg are inadvertent contaminants of refined GaP (Sec. IIA). The cleanest Mg no-phonon lines [Fig. 11(c)] were obtained from Mg_3N_2-doped solution-grown crystals for which the lower-energy Mg-exciton structure was obscured by Mg-S pair luminescence (Ref. 10). Figure 7 was obtained from a crystal in which Mg and a very small amount of C appeared inadvertently in attempts to dope with Ca. Usually, relatively much more C was present in spectra from our Ca- and Ba-doped crystals than in Fig. 7. Care is needed in the distinction between Mg- and C-exciton components, because component C_1^0 lies below Mg_2^0 by only 0.05 meV, while C_2^0 and Mg_3^0 are essentially isoenergetic (to within ± 0.01 meV). The presence of C may be deduced from these small energy differences in sharp spectra, from intensity anomalies within this group of lines (higher-energy components too strong for a pure Mg spectrum), from the presence of the characteristic higher-energy C no-phonon lines at high-excitation intensities [Fig. 11(d)], or from anomalous intensity distributions among the MC phonon replicas due to the large difference in no-phonon strength of the C and Mg excitons (Fig. 9).

[20]For the acceptor Be see P. J. Dean and M. Ilegems, Bull Am. Phys. Soc. 15, 1342 (1970).

[21]P. J. Dean, J. D. Cuthbert, D. G. Thomas, and R. T. Lynch, Phys. Rev. Letters 18, 122 (1967).

[22]C. H. Henry, J. J. Hopfield, and L. C. Luther, Phys. Rev. Letters 17, 1178 (1966).

[23]D. D. Manchon, Jr. and P. J. Dean, in *Proceedings of the International Conference on Physics of Semiconductors, Cambridge*, 1970 (U. S. Atomic Energy Commission, Oak Ridge, 1970), p. 760.

[24]T. N. Morgan, Phys. Rev. Letters 21, 819 (1968).

[25]P. J. Dean, J. R. Haynes, and W. F. Flood, Phys. Rev. 161, 711 (1967).

[26]T. N. Morgan (private communication).

[27]T. N. Morgan, Phys. Rev. Letters 24, 887 (1970).

[28]Y. Yafet and D. G. Thomas, Phys. Rev. 131, 2405 (1963).

[29]J. L. Merz, R. A. Faulkner, and P. J. Dean, Phys. Rev. 188, 1228 (1969).

[30]C. H. Henry, P. J. Dean, and J. D. Cuthbert, Phys. Rev. 166, 754 (1968).

[31]P. J. Dean and D. G. Thomas, Phys. Rev. 150, 690 (1966).

[32]A. N. Pikhtin and D. A. Yas'kov, Fiz. Tverd. Tela 11, 2213 (1969) [Sov. Phys. Solid State 11, 1787 (1970)].

[33]K. P. Sinha and M. DiDomenico, Jr., Phys. Rev. B 1, 2623 (1970).

[34]P. J. Dean and C. H. Henry, Phys. Rev. 176, 928 (1968).

[35]M. L. Cohen and T. K. Bergstresser, Phys. Rev. 141, 789 (1966).

[36]D. G. Thomas and J. J. Hopfield, Phys. Rev. 150, 680 (1966).

[37]A. T. Vink and R. C. Peters, J. Luminescence 3, 209 (1970).

[38]W. Schairer (private communication).